Principles of discrete time mechanics: III. Quantum field theory

Principles of discrete time mechanics: III. Quantum field theory

Keith Norton and George Jaroszkiewicz

† Department of Mathematics, University of Nottingham, University Park, Nottingham NG7 2RD, UK

Abstract.   We apply the principles discussed in earlier papers to the construction of discrete time quantum field theories. We discuss some of the issues concerned with the loss of Lorentz covariance and its recovery in the appropriate limit. We use the Schwinger action principle to find the discrete time free field commutators for scalar fields, which allows us to set up the reduction formalism for discrete time scattering processes. Then we derive the discrete time analogue of the Feynman rules for a scalar field with a cubic self-interaction and give examples of discrete time scattering amplitude calculations. We find overall conservation of total linear momentum and overall conservation of total θ parameters, which is the discrete time analogue of energy conservation and corresponds to the existence of a Logan invariant for the system. We find that temporal discretization leads to softened vertex factors, modifies propagators and gives a natural cut-off for physical particle momenta.

1. Introduction

This paper is the third in a series devoted to the construction of discrete time classical and quantum mechanics, based on the notion that there is a fundamental interval of time, T. The objective is to investigate the properties of a dynamics where continuity in time, and hence differentiability with respect to time, has been abolished. With no velocities, there are no Lagrangians in the ordinary sense, and then there are neither canonical conjugate momenta nor Hamiltonians. It would then appear to be a catastrophic method for recasting the laws of classical and quantum physics, but as we try to show in this paper, this is not really the case. Moreover, there is every prospect of finding novel features of the dynamics not encountered in continuous time mechanics which may go some way towards alleviating the divergence problems encountered in conventional quantum field theory.

The first paper of this series, referred to as *paper I* [1], introduced basic principles for the temporal discretization of continuous time classical and quantum particle mechanics. The second paper, referred to as *paper II* [2], applied these principles to classical field theory, including gauge invariant electrodynamics and the Dirac field. These papers should be consulted for further explanation of our notation and methodology. In this paper, referred to as *paper III*, we apply the techniques of *paper I* to the quantization of the scalar field systems studied in *paper II*, i.e. we discuss quantized discrete time scalar field theory.

Following the analysis of the earlier papers, we denote by $\mathcal{D}$ our process of discretizing time using virtual paths and by $\mathcal{Q}$ the process of quantization using transition amplitudes based on the system function, each of these processes being applied to some classical Lagrangian L. Then we can say that *paper I* discusses models of type $\mathcal{D}L$ and $\mathcal{Q}\mathcal{D}L$

whereas *paper II* discusses models of type $\mathcal{DL}$, where $\mathcal{L}$ is a Lagrange density. Now since such a density may be associated with the first quantization of a classical theory, i.e. to $\mathcal{QL}$ models, as discussed in *paper II* for the Schrödinger equation, models of type $\mathcal{DL}$ may be regarded as equivalent in some sense to those of type $\mathcal{DQL}$. This allows a direct comparison of the processes $\mathcal{DQ}$ and $\mathcal{QD}$, and in *paper II* it was argued that these are not the same in general.

This paper considers models of type $\mathcal{QDL}$. Because such models may be regarded as equivalent in the above sense to those of type $\mathcal{QDQL}$, then *paper III* may be considered to be a discussion of discrete time second quantization. Note, however, that the $\mathcal{QDQ}$ process used in this paper is not in general equivalent to the process $\mathcal{DQQ}$ because the $\mathcal{D}$ and $\mathcal{Q}$ processes do not commute. This means that our paper discusses the quantization of discrete time classical field theories and not the temporal discretization of quantum field theories, such as in lattice gauge theories. In the latter, discretization is regarded as an approximation which becomes exact in the continuum limit. In our approach our mechanics is regarded as exact at each stage and the continuum limit is taken only to make comparisons with standard formulations. This is a significant difference between our approach and various other formulations using a discrete time, because of our insistence on adhering to the principles of the formulation at all stages. In particular, the constants of motion are constructed to be exact and not approximately conserved up to some powers of T.

An important question which arises naturally in the context of discrete time and/or space mechanics is that of Lorentz covariance. Our answer is that Lorentz symmetry of say scattering matrix elements emerges in the appropriate limit, such as $T \to 0$, and other than that, is not really something to worry about, as it is regarded here as an approximation to a deeper underlying structure. An analogy with representational art is useful here. If we liken continuous time theories to pictures drawn on normal canvas, then our discrete time mechanics is a picture drawn on a conventional analogue television screen. In the former model of spacetime it is frequently speculated that continuity might break down, perhaps at Planck scales (we do know that a real canvas is made up of atoms), but otherwise, continuity on the plane of the canvas exists at all levels and carries with it all the associated symmetries of the plane, such as translation and rotational invariance. On a television screen, however, we have two perspectives. From a distance, a television picture really does look like one painted on a canvas, but a closer look would readily show the horizontal lines which make up the picture. There is a discreteness vertically, but a continuity horizontally. Likewise, in discrete time mechanics, there is a discreteness along the time axis with all the normal continuity along the space axis. Like a television picture, there is less symmetry when viewed close up than when viewed at a distance, and it would be futile and in principle wrong to try to pretend that such long-distance symmetries should exist at all scales. What we are doing, therefore, is more like exploring the mechanics of a television set rather than the pictures drawn on it. This suggests that discretization of time in the context of general relativity is an obvious candidate for investigation.

The art analogy can be pursued further. Discretisation of space as well as time, such as in lattice gauge theories and the work of authors such as Bender *et al* [3] and Yamamoto *et al* [4], gives a lattice spacetime picture which corresponds to what occurs on a computer monitor, where the picture is fully digitized. This form of discrete spacetime mechanics is inherently different to our discrete time mechanics and the two should not be confused.

Another important question related to the issue of Lorentz covariance is: *In which inertial frame are we discretizing time?* Of course, if we believed in an absolute time in the strict sense of Newton then we would have an immediate answer. However, we

are approaching discrete time from a more modern perspective and the problem is a very real one for us. Our answer is to go beyond special relativity and consider cosmological perspectives. It is an empirical fact that, from the point of view of observers on the earth, we are moving at a speed of about 500–600 km s^{-1} relative to a frame of reference in which the cosmic background radiation field of Penzias and Wilson is isotropic [5] (the so-called *dipole effect*). According to the cosmological principle, we should be able to find a local inertial frame in the neighbourhood of each point in space time with the same property, i.e. one in which the cosmic background radiation field is isotropic to a very high degree, except for tiny ripples equivalent to those recently observed by COBE [6]. This frame should be unique at each point, up to spatial rotations. We will refer to this frame as the *local absolute frame*.

If we let our universe be reasonably well described via a Robertson–Walker metric, then as we change position and time we expect the local absolute frame to change as well. However, it will always be empirically identifiable at each place and time in the universe. The standard coordinate time in such a frame is called the proper or comoving time in the usual formulation of Robertson–Walker cosmology, and represents the proper time of a point particle (or galaxy) at rest relative to the local cosmic mass distribution. In answer to the question posed above, we suggest that time is discretized via local absolute frames.

Care should be taken to keep in mind that throughout this paper, when we discuss Minkowski spacetime and its temporal discretization, we are really referring to local inertial frames. Of course, there is the additional question of local variations due to gravitational disturbances arising from locally inhomogeneous matter densities. Answering this question amounts to constructing a discrete time analogue of general relativity, which will be reserved for a subsequent paper in this series. Since we are interested in applications to particle theory in this paper, we will not consider these issues further here, except to make a final observation about this line of thought. If we were discretizing space as well as time (which we are not), we would have to consider the additional question: *How are we discretizing space?* If we were choosing the simplest sort of discretization scheme, a cubic lattice (say), then we would have to specify three spatial orthogonal Cartesian axes. Until recently there was no evidence of any spatial anisotropy on truly cosmological scales, so we had no criterion for picking out any special directions in space. We note, however, the very recent observation of the so-called *corkscrew effect* reported by Nodland and Ralston [7], which if confirmed will require a re-assessment of the position. The comic background radiation field, however, *does* give us a working prescription for picking out a unique timelike direction at each point.

Because of the relatively greater complexity of discrete time field theory compared with conventional field theory, in this paper we have restricted our attention to scalar fields. The general features found here should find their direct analogues with the Dirac and Maxwell fields. We reserve the further discussion of these fields to the next papers in this series. Our principal aim in this paper is to discuss how the process of discretizing time alters Feynman rules for scattering amplitudes and scattering cross sections. Issues of renormalization are left for later papers in the series. An important feature of the present investigation is the discrete time oscillator, which is directly related to free particle states used to define *in* and *out* states.

In section 2 we discuss the quantization of scalar fields, using Schwinger's action principle to derive ground-state expectation values of time ordered products. Then in section 3 we apply these methods to the free neutral scalar field. The results are in agreement with the more direct calculation of the quantized discrete time harmonic oscillator discussed in *paper I*. We examine in more detail the free scalar field propagator and the free field

commutators, the results being consistent with the vacuum expectation values discussed previously. We find that the free particle creation and annihilation operators have a natural cut-off in physical particle state momenta, corresponding to what we call the *elliptic* regime. Although it is possible to construct linear invariants of the motion outside this regime, states associated with such operators have various expectation values which diverge or tend to zero in the infinite time limit, and this makes them unsuitable for representing physical particles. If T is the fundamental time interval and the discrete time analogue of energy E is defined by $E = \sqrt{\boldsymbol{p} \cdot \boldsymbol{p} + m^2}$ in natural units (where $c = \hbar = 1$), then our formulation leads to the condition $TE < \sqrt{12}$ for physical *in* or *out* particles, which we call the *parabolic barrier*. This barrier manifests itself in a number of ways. For example, the particle flux density associated with each creation operator is found to be modified by a factor $\sqrt{1 - T^2E^2/12}$, which makes physical sense only in the elliptic regime.

  We then turn to interacting scalar fields theories. In section 4 we set up the discrete time reduction formulae needed to calculate scattering cross sections and then discuss the perturbative expansion of the vacuum expectation values of discrete time-ordered products for a specific example, φ^3 scalar field theory. We give the discrete time analogues of the Feynman rules in configuration space and in momentum space. In section 5 we present a scattering calculation for the box diagram to illustrate the formalism and then give general rules for scattering amplitudes. Finally, in section 6 we give a number of applications of our scattering amplitude rules. We find that in each case there is a conserved quantity in scattering processes analogous to energy, related to the existence of what we call a Logan invariant of the system function. Fortunately, the LSZ formalism is powerful enough to reveal the existence of such a Logan invariant in a scattering process without the need to find it explicitly for the fully interacting system.

  Our analysis reveals that for φ^3 interactions our discrete time Feynman rules involve vertex softening in the basic diagrams, before any renormalization effects are considered. This may be a significant feature of more realistic interactions. Also, the propagators associated with internal lines are modified and we use them to show how Lorentz covariance can emerge as an approximate symmetry of the mechanics. There is therefore some prospect of our programme making some progress towards the alleviation, if not complete removal, of divergences in the traditional renormalization programme of continuous time relativistic quantum field theory.

2. The discrete time quantized scalar field

We turn now to the quantization of the neutral scalar field. Following the methodology and notation discussed in *papers I* and II, particularly the discussion in *paper I* on the quantized inhomogeneous oscillator, the discrete time system function for a system with a scalar field φ degree of freedom coupled to a source j is chosen to be given by

$$F^n[j] = F^n + \tfrac{1}{2} T \int \mathrm{d}^3 \boldsymbol{x} \, \{ j_{n+1} \varphi_{n+1} + j_n \varphi_n \} \tag{1}$$

where $F^n \equiv \int \mathrm{d}^3 \boldsymbol{x} \, \mathcal{F}^n$ is the system function in the absence of the source. There are other ways of introducing sources into the system, but the above method was found to be most practical. Since these sources are eventually switched off, it does not really matter how they are introduced, as long as they are dealt with consistently according to the principles of discrete time mechanics.

With the above system function the Cadzow equation of motion [2, 8] is

$$\frac{\delta}{\delta\varphi_n(\boldsymbol{x})}\{F^n + F^{n-1}\} + Tj_n(\boldsymbol{x}) \underset{c}{=} 0 \tag{2}$$

which reduces to

$$\frac{\partial}{\partial\varphi_n}\{\mathcal{F}^n + \mathcal{F}^{n-1}\} - \nabla\cdot\frac{\partial}{\partial\nabla\varphi_n}\{\mathcal{F}^n + \mathcal{F}^{n-1}\} + Tj_n \underset{c}{=} 0 \tag{3}$$

where $\mathcal{F}^n$ is the system function density in the absence of sources. Here we use the symbol $\underset{c}{=}$ to denote an equality holding over a true or dynamical classical trajectory.

The action sum $A^{NM}[j]$ in the presence of sources for evolution between times MT and NT is

$$A^{NM}[j] = A^{NM} + \tfrac{1}{2}T\int \mathrm{d}^3\boldsymbol{x}\,\{j_M\varphi_M + j_N\varphi_N\} + T\sum_{n=M+1}^{N-1}\int \mathrm{d}^3\boldsymbol{x}\,j_n\varphi_n \qquad M < N. \tag{4}$$

Use of the discrete time Schwinger action principle [1]

$$\delta\langle\phi, N|\psi, M\rangle^j = \mathrm{i}\langle\phi, N|\delta\hat{A}^{NM}[j]|\psi, M\rangle^j \qquad M < N \tag{5}$$

leads to the functional derivatives

$$\frac{-\mathrm{i}}{T}\frac{\delta}{\delta j_M(\boldsymbol{x})}\langle\phi, N|\psi, M\rangle^j = \frac{1}{2}\langle\phi, N|\hat{\varphi}_M(\boldsymbol{x})|\psi, M\rangle^j$$

$$\frac{-\mathrm{i}}{T}\frac{\delta}{\delta j_n(\boldsymbol{x})}\langle\phi, N|\psi, M\rangle^j = \langle\phi, N|\hat{\varphi}_n(\boldsymbol{x})|\psi, M\rangle^j \qquad M < n < N \tag{6}$$

$$\frac{-\mathrm{i}}{T}\frac{\delta}{\delta j_N(\boldsymbol{x})}\langle\phi, N|\psi, M\rangle^j = \frac{1}{2}\langle\phi, N|\hat{\varphi}_N(\boldsymbol{x})|\psi, M\rangle^j.$$

Also, we find

$$\frac{-\mathrm{i}}{T}\frac{\delta}{\delta j_n(\boldsymbol{x})}\frac{-\mathrm{i}}{T}\frac{\delta}{\delta j_m(\boldsymbol{y})}\langle\phi, N|\psi, M\rangle^j = \langle\phi, N|\hat{\varphi}_m(\boldsymbol{y})\hat{\varphi}_n(\boldsymbol{x})|\psi, M\rangle^j[\Theta_{m-n} + \tfrac{1}{2}\delta_{m-n}]$$

$$+\langle\phi, N|\hat{\varphi}_n(\boldsymbol{x})\hat{\varphi}_m(\boldsymbol{y})|\psi, M\rangle^j[\Theta_{n-m} + \tfrac{1}{2}\delta_{m-n}] \qquad (M < m, n < N) \tag{7}$$

where Θ_n and δ_n are the discrete time step function and discrete time delta defined in *paper I*. We will write (7) in the form

$$\frac{-\mathrm{i}}{T}\frac{\delta}{\delta j_n(\boldsymbol{x})}\frac{-\mathrm{i}}{T}\frac{\delta}{\delta j_m(\boldsymbol{y})}\langle\phi, N|\psi, M\rangle^j = \langle\phi, N|\tilde{T}\hat{\varphi}_n(\boldsymbol{x})\hat{\varphi}_m(\boldsymbol{y})|\psi, M\rangle^j \qquad (M < m, n < N) \tag{8}$$

where $\tilde{T}$ denotes discrete time ordering as discussed in *paper I*.

In applications we will normally be interested in the scattering limit $N = -M \to \infty$ and in matrix elements involving the in and out vacua. We shall restrict our calculations to such matters. This means we will discuss the r-point functions defined by

$$G^j_{n_1n_2...n_r}(\boldsymbol{x}_1, \ldots, \boldsymbol{x}_r) = \frac{\langle 0^{\mathrm{out}}|\tilde{T}\hat{\varphi}_{n_1}(\boldsymbol{x}_1)\ldots\hat{\varphi}_{n_r}(\boldsymbol{x}_r)|0^{\mathrm{in}}\rangle^j}{\langle 0^{\mathrm{out}}|0^{\mathrm{in}}\rangle^j}$$

$$= \frac{1}{Z[j]}\frac{-\mathrm{i}\delta}{T\delta j_{n_1}(\boldsymbol{x}_1)}\cdots\frac{-\mathrm{i}\delta}{T\delta j_{n_r}(\boldsymbol{x}_r)}Z[j] \tag{9}$$

where

$$Z[j] = \langle 0^{\mathrm{out}}|0^{\mathrm{in}}\rangle^j \tag{10}$$

is the ground-state (vacuum) functional in the presence of the sources and $\tilde{T}$ denotes discrete time ordering.

An important question here concerns the existence of the ground state. Similarly to most continuous time field theories, we have no general proof that a ground state exists for interacting discrete time field theories. Moreover, in discrete time mechanics there is no Hamiltonian as such, so the question becomes more acute. However, for free fields, there will be what we refer to as a compatible operator corresponding to some appropriate Logan invariant [1, 10]. This is the nearest analogue to the Hamiltonian in continuous time theory. Moreover, the appropriate compatible operator for free neutral scalar fields is positive definite and this allows a meaning for the in and out vacua to be given.

3. The discrete time free scalar field

3.1. The free scalar field propagator

Given the continuous time Lagrange density

$$\mathcal{L}_0 = \tfrac{1}{2}\partial_\mu\varphi\partial^\mu\varphi - \tfrac{1}{2}\mu^2\varphi^2 \tag{11}$$

we use the virtual path approach discussed in [2] to find the system function density

$$\mathcal{F}_0^n = \frac{(\varphi_{n+1} - \varphi_n)^2}{2T} - \frac{T}{6}(\nabla\varphi_{n+1}^2 + \nabla\varphi_{n+1}\cdot\nabla\varphi_n + \nabla\varphi_n^2) - \frac{\mu^2 T}{6}(\varphi_{n+1}^2 + \varphi_{n+1}\varphi_n + \varphi_n^2). \tag{12}$$

In the presence of the sources we take

$$F_0^n[j] = F_0^n + \tfrac{1}{2}T\int d^3x\,\{j_{n+1}\varphi_{n+1} + j_n\varphi_n\} \tag{13}$$

and then the Cadzow equation of motion is

$$\frac{\varphi_{n+1} - 2\varphi_n + \varphi_{n-1}}{T^2} + (\mu^2 - \nabla^2)\frac{(\varphi_{n+1} + 4\varphi_n + \varphi_{n-1})}{6} \underset{c}{=} j_n. \tag{14}$$

We now define the spatial Fourier transforms

$$\tilde{\varphi}_n(\mathbf{p}) \equiv \int d^3x\,e^{-i\mathbf{p}\cdot\mathbf{x}}\varphi_n(\mathbf{x})$$

$$\tilde{j}_n(\mathbf{p}) \equiv \int d^3x\,e^{-i\mathbf{p}\cdot\mathbf{x}}j_n(\mathbf{x}) \tag{15}$$

and then the equation of motion becomes

$$\left\{\frac{(U_n - 2 + U_n^{-1})}{T^2} + E^2\frac{(U_n + 4 + U_n^{-1})}{6}\right\}\tilde{\varphi}_n(\mathbf{p}) \underset{c}{=} \tilde{j}_n(\mathbf{p}) \tag{16}$$

where $E \equiv \sqrt{\mathbf{p}\cdot\mathbf{p} + \mu^2}$ and U_n is the classical temporal displacement operator defined by

$$U_n f_n \equiv f_{n+1} \tag{17}$$

for any variable indexed by n. The solution to (16) with Feynman scattering boundary conditions is

$$\tilde{\varphi}_n(\mathbf{p}) = \tilde{\varphi}_n^{(0)}(\mathbf{p}) - T\sum_{m=-\infty}^{\infty}\tilde{\Delta}_F^{n-m}(\mathbf{p})\tilde{j}_m(\mathbf{p}) \tag{18}$$

where $\tilde{\varphi}_n^{(0)}(\boldsymbol{p})$ is a solution to the homogeneous equation

$$\{\frac{(U_n - 2 + U_n^{-1})}{T^2} + E^2 \frac{(U_n + 4 + U_n^{-1})}{6}\}\tilde{\varphi}_n^{(0)}(\boldsymbol{p}) = 0 \tag{19}$$

and $\tilde{\Delta}_F^n(\boldsymbol{p})$ is the discrete time Feynman propagator in momentum space satisfying the equation

$$\left\{\frac{(U_n - 2 + U_n^{-1})}{T^2} + E^2 \frac{(U_n + 4 + U_n^{-1})}{6}\right\} \tilde{\Delta}_F^n(\boldsymbol{p}) = -\frac{\delta_n}{T}. \tag{20}$$

This equation for the propagator may be written in the form

$$\{U_n - 2\eta_E + U_n^{-1}\}\tilde{\Delta}_F^n(\boldsymbol{p}) = -\Gamma_E \delta_n \tag{21}$$

where

$$\Gamma_E = \frac{6T}{6 + T^2 E^2} \qquad \eta_E = \frac{6 - 2T^2 E^2}{6 + T^2 E^2}. \tag{22}$$

Using our experience with the discrete time harmonic oscillator propagator discussed in *paper I*, we may immediately write down the solution for the propagator in the form

$$\tilde{\Delta}_F^n(\boldsymbol{p}) = \frac{\Gamma_E}{2\mathrm{i}\sin\theta_E}\mathrm{e}^{-\mathrm{i}|n|\theta_E} = \frac{\Gamma_E}{2\mathrm{i}\sin\theta_E}\{\mathrm{e}^{-\mathrm{i}n\theta_E}\Theta_n + \delta_n + \mathrm{e}^{\mathrm{i}n\theta_E}\Theta_{-n}\} \tag{23}$$

where $\eta_E = \cos\theta_E$. As discussed in *paper I*, this expression holds for the elliptic and hyperbolic regimes with suitable analytic continuation. In the continuous time limit $T \to 0$, $nT \to t$, we recover the usual Feynman propagator in a spatially Fourier transformed form, namely

$$\lim_{T\to 0, n\to\infty, nT=t}\tilde{\Delta}_F^n(\boldsymbol{p}) = -\frac{\mathrm{i}}{2E}\{\mathrm{e}^{-\mathrm{i}tE}\theta(t) + \mathrm{e}^{\mathrm{i}tE}\theta(-t)\}$$

$$= \int \frac{\mathrm{d}\omega}{2\pi} \frac{\mathrm{e}^{-\mathrm{i}\omega t}}{\omega^2 - \boldsymbol{p}\cdot\boldsymbol{p} - \mu^2 + \mathrm{i}\epsilon}$$

$$= \tilde{\Delta}_F(\boldsymbol{p}, t) = \int \mathrm{d}^3x\,\mathrm{e}^{-\mathrm{i}\boldsymbol{p}\cdot\boldsymbol{x}}\Delta_F(\boldsymbol{x}, t). \tag{24}$$

Turning to the quantization process, the functional derivative satisfies the rule

$$\frac{\delta}{\delta j_n(\boldsymbol{x})} j_m(\boldsymbol{y}) = \delta_{n-m}\delta^3(\boldsymbol{x} - \boldsymbol{y}). \tag{25}$$

With the definition

$$\frac{\delta}{\delta \tilde{j}_n(\boldsymbol{p})} \equiv \frac{1}{(2\pi)^3} \int \mathrm{d}^3x\,\mathrm{e}^{\mathrm{i}\boldsymbol{p}\cdot\boldsymbol{x}}\frac{\delta}{\delta j_n(\boldsymbol{x})} \tag{26}$$

we find

$$\frac{\delta}{\delta \tilde{j}_n(\boldsymbol{p})} \tilde{j}_m(\boldsymbol{q}) = \delta_{n-m}\delta^3(\boldsymbol{p} - \boldsymbol{q}) \tag{27}$$

and then

$$\langle 0^{\mathrm{out}}|\varphi_n(\boldsymbol{x})|0^{\mathrm{in}}\rangle^j = -\frac{\mathrm{i}}{T}\frac{\delta}{\delta j_n(\boldsymbol{x})}Z[j] \tag{28}$$

gives

$$\langle 0^{\mathrm{out}}|\tilde{\varphi}_n(\boldsymbol{p})|0^{\mathrm{in}}\rangle^j = -\frac{\mathrm{i}(2\pi)^3}{T}\frac{\delta}{\delta \tilde{j}_n(-\boldsymbol{p})}Z[j]. \tag{29}$$

Hence we find

$$Z_0[j] = Z_0[0]\exp\left\{-\tfrac{1}{2}\mathrm{i}T^2\sum_{n,m=-\infty}^{\infty}\int \mathrm{d}^3x\,\mathrm{d}^3y\,j_n(\boldsymbol{x})\Delta_F^{n-m}(\boldsymbol{x}-\boldsymbol{y})j_m(\boldsymbol{y})\right\} \tag{30}$$

where

$$\Delta_F^n(\boldsymbol{x}) = \int \frac{\mathrm{d}^3p}{(2\pi)^3}\mathrm{e}^{\mathrm{i}\boldsymbol{p}\cdot\boldsymbol{x}}\tilde{\Delta}_F^n(\boldsymbol{p}). \tag{31}$$

This propagator satisfies the equation

$$\left\{\frac{U_n - 2 + U_n^{-1}}{T^2} + (\mu^2 - \nabla^2)\frac{(U_n + 4 + U_n^{-1})}{6}\right\}\Delta_F^n(\boldsymbol{x}) = -\frac{\delta_n}{T}\delta^3(\boldsymbol{x}). \tag{32}$$

3.2. The free field commutators

In this section we use (30) to obtain the vacuum expectation value of the free field commutators. Writing the propagator (23) in the form

$$\tilde{\Delta}_F^n(\boldsymbol{p}) = c_E[z^{-n}\Theta_n + \delta_n + z^n\Theta_{-n}] \tag{33}$$

we then find for the elliptic and hyperbolic regimes

$$\begin{aligned}c_E &= \frac{-\mathrm{i}\sqrt{3}}{E\sqrt{12 - T^2E^2}} & TE < \sqrt{12}\\[2mm] &= \frac{-3}{E\sqrt{T^2E^2 - 12}} & TE > \sqrt{12}.\end{aligned} \tag{34}$$

An application of (9) gives

$$\langle 0|\hat{\varphi}_{n+1}(\boldsymbol{x})\hat{\varphi}_n(\boldsymbol{y})|0\rangle = \mathrm{i}\Delta_F^1(\boldsymbol{x}-\boldsymbol{y}) \tag{35}$$

from which we deduce

$$\begin{aligned}\langle 0|[\hat{\varphi}_{n+1}(\boldsymbol{x}),\hat{\varphi}_n(\boldsymbol{y})]|0\rangle &= -6\mathrm{i}T\int \frac{\mathrm{d}^3p}{(2\pi)^3}\frac{\mathrm{e}^{\mathrm{i}\boldsymbol{p}\cdot(\boldsymbol{x}-\boldsymbol{y})}}{6 + (\boldsymbol{p}\cdot\boldsymbol{p}+\mu^2)T^2}\\[2mm] &= \frac{-6\mathrm{i}}{4\pi T|\boldsymbol{x}-\boldsymbol{y}|}\mathrm{e}^{-\sqrt{\mu^2+6/T^2}|\boldsymbol{x}-\boldsymbol{y}|}.\end{aligned} \tag{36}$$

Both elliptic and hyperbolic regions of momentum space contribute to this result, which has the form of a Yukawa potential function.

We now turn to the direct approach to quantization discussed in *paper I*. If we define the momentum $\pi_n(\boldsymbol{x})$ conjugate to $\varphi_n(\boldsymbol{x})$ via the rule $\pi_n(\boldsymbol{x}) \equiv -\frac{\delta}{\delta\varphi_n(\boldsymbol{x})}F^n$ then (12) gives

$$\pi_n \equiv \frac{\varphi_{n+1}-\varphi_n}{T} + \frac{T}{6}(\mu^2 - \nabla^2)(\varphi_{n+1}+2\varphi_n) \tag{37}$$

for the free field. The naive canonical quantization discussed in *paper I* is equivalent in field theory terms to

$$[\hat{\pi}_n(\boldsymbol{x}),\hat{\varphi}_n(\boldsymbol{y})] = -\mathrm{i}\delta^3(\boldsymbol{x}-\boldsymbol{y}) \tag{38}$$

from which we deduce

$$\begin{aligned}[\hat{\varphi}_{n+1}(\boldsymbol{x}),\hat{\varphi}_n(\boldsymbol{y})] &= -6\mathrm{i}T\int \frac{\mathrm{d}^3p}{(2\pi)^3}\frac{\mathrm{e}^{\mathrm{i}\boldsymbol{p}\cdot(\boldsymbol{x}-\boldsymbol{y})}}{6 + (\mu^2+\boldsymbol{p}\cdot\boldsymbol{p})T^2}\\[2mm] &= \frac{-6\mathrm{i}}{4\pi T|\boldsymbol{x}-\boldsymbol{y}|}\mathrm{e}^{-\sqrt{\mu^2+6/T^2}|\boldsymbol{x}-\boldsymbol{y}|}\end{aligned} \tag{39}$$

assuming $[\hat{\varphi}_n(\boldsymbol{x}), \hat{\varphi}_n(\boldsymbol{y})] = 0$. This is consistent with the approach to quantization via the Schwinger action principle from which we obtained (36).

We note that the reason this works is that the system function for a free field is an example of what we call a *normal system* in *paper I*. For interacting field theories this will no longer be the case and then the commutators analogous to the above will probably no longer be *c*-functions. We recall that in continuous time field theories, interacting field commutators are not canonical in general either, so the analogies between discrete and continuous time mechanics also hold well here.

For the free field particle creation and annihilation operators we define the variables

$$a_n(\boldsymbol{p}) = i\Gamma_E^{-1} e^{in\theta_E} [\tilde{\varphi}_{n+1}(\boldsymbol{p}) - e^{i\theta_E} \tilde{\varphi}_n(\boldsymbol{p})] \tag{40}$$

where

$$\Gamma_E = \frac{6T}{6 + T^2 E^2} \qquad \tilde{\varphi}_n(\boldsymbol{p}) = \int d^3x\, e^{-i\boldsymbol{p}\cdot\boldsymbol{x}} \varphi_n(\boldsymbol{x}) \tag{41}$$

and the momentum $\boldsymbol{p}$ is restricted to the elliptic region. Then we find

$$[\hat{a}_n(\boldsymbol{p}), \hat{a}_n^+(\boldsymbol{q})] = 2E\sqrt{1 - T^2 E^2/12}\,(2\pi)^3 \delta^3(\boldsymbol{p} - \boldsymbol{q}) \tag{42}$$

when we quantize and use (39). This tends to the correct continuous time limit as $T \to 0$.

If we interpret the factor $2E\sqrt{1 - T^2 E^2/12}$ in the above as a particle flux density then this will be indistinguishable from the conventional density $2E$ in continuous time field theory for normal momenta, but falls to zero as the parabolic barrier $TE = \sqrt{12}$ is approached from below. This suggests that there is in principle a physical limit to the possibility of creating extremely high momentum particle states in the laboratory or of observing such particles in cosmic rays. This should have an effect on all discussions involving momentum space, such as particle decay lifetime and cross section calculations, and in the long term, on unified field theories.

4. Interacting discrete time scalar fields

4.1. Reduction formulae

In applications to particle scattering theory we shall be interested in incoming and outgoing physical particle states, with individual particle energies satisfying the elliptic condition $TE < \sqrt{12}$. We note that energy is defined here via the linear momentum $\boldsymbol{p}$ by the rule

$$E \equiv +\sqrt{\boldsymbol{p}\cdot\boldsymbol{p} + \mu^2}. \tag{43}$$

This is the *only* meaning we give to the term *energy*.

Given the annihilation and creation operators

$$\hat{a}_n(\boldsymbol{p}) = i\Gamma_E^{-1} \int d^3x\, e^{in\theta_E - i\boldsymbol{p}\cdot\boldsymbol{x}} [\hat{\varphi}_{n+1}(\boldsymbol{x}) - e^{i\theta_E} \hat{\varphi}_n(\boldsymbol{x})]$$

$$\hat{a}_n^+(\boldsymbol{p}) = -i\Gamma_E^{-1} \int d^3x\, e^{-in\theta_E + i\boldsymbol{p}\cdot\boldsymbol{x}} [\hat{\varphi}_{n+1}(\boldsymbol{x}) - e^{-i\theta_E} \hat{\varphi}_n(\boldsymbol{x})] \tag{44}$$

where

$$\Gamma_E = \frac{6T}{6 + T^2 E^2} \qquad \cos\theta_E \equiv \eta_E = \frac{6 - 2T^2 E^2}{6 + T^2 E^2} \tag{45}$$

then a direct application of the standard reduction formalism gives the reduced matrix elements

$$\langle \alpha^{\text{out}} | (\tilde{T}\hat{\zeta}) \hat{a}_{\text{in}}^+(\boldsymbol{p}) | \beta^{\text{in}} \rangle_R = i \sum_{n=-\infty}^{\infty} \int d^3x\, e^{-in\theta_E + i\boldsymbol{p}\cdot\boldsymbol{x}} \overrightarrow{K_{n,p}} \langle \alpha^{\text{out}} | \tilde{T}\hat{\zeta} \hat{\varphi}_n(\boldsymbol{x}) | \beta^{\text{in}} \rangle \tag{46}$$

and

$$\langle \alpha^{\text{out}} | \hat{a}_{\text{out}}(\boldsymbol{p}) \tilde{T} \hat{\zeta} | \beta^{\text{in}} \rangle_R = \mathrm{i} \sum_{n=-\infty}^{\infty} \int \mathrm{d}^3 \boldsymbol{x} \, \mathrm{e}^{\mathrm{i} n \theta_E - \mathrm{i} \boldsymbol{p} \cdot \boldsymbol{x}} \overrightarrow{K_{n,\boldsymbol{p}}} \langle \alpha^{\text{out}} | \tilde{T} \hat{\zeta} \hat{\varphi}_n(\boldsymbol{x}) | \beta^{\text{in}} \rangle \tag{47}$$

where $\hat{\zeta}$ denotes any collection of field operators and

$$\overrightarrow{K_{n,\boldsymbol{p}}} \equiv \Gamma_E^{-1} (U_n - 2\eta_E + U_n^{-1}). \tag{48}$$

Using these results we can readily write down the scattering matrix for a process consisting of r incoming physical momentum particles with momenta $\boldsymbol{p}_1, \boldsymbol{p}_2, \ldots, \boldsymbol{p}_r$ and s outgoing particles with momenta $\boldsymbol{q}_1, \boldsymbol{q}_2, \ldots, \boldsymbol{q}_s$.

4.2. Interacting fields: scalar field theory

We turn now to interacting scalar field theories based on continuous time Lagrange densities of the form

$$\mathcal{L} = \mathcal{L}_0 - V(\varphi). \tag{49}$$

In order to illustrate what happens in discrete time quantum field theory, we shall discuss the details of a scalar field with a φ^3 interaction term, deriving the analogue of the Feynman rules.

In the presence of sources the above Lagrange density leads to the system function

$$F^n[j] = F^n_{(0)} - T \int_0^1 \mathrm{d}\lambda \int \mathrm{d}^3 \boldsymbol{x} \, V(\tilde{\varphi}_n) + \tfrac{1}{2} T \int \mathrm{d}^3 \boldsymbol{x} \, \{ j_n \varphi_n + j_{n+1} \varphi_{n+1} \} \tag{50}$$

where we use the virtual paths

$$\tilde{\varphi}_n(\boldsymbol{x}) \equiv U_n^\lambda \varphi(\boldsymbol{x}) = \lambda \varphi_{n+1}(\boldsymbol{x}) + \bar{\lambda} \varphi_n(\boldsymbol{x}) \qquad 0 \leqslant \lambda \leqslant 1 \qquad \bar{\lambda} \equiv 1 - \lambda \tag{51}$$

as discussed in *paper II* for neutral scalar fields. Here and below we shall find the operator

$$U_n^\lambda \equiv \lambda U_n + \bar{\lambda} \tag{52}$$

particularly useful, where U_n is the classical temporal displacement operator defined by (17). The vacuum functional is now defined via the discrete time path integral

$$Z[j] = \int [\mathrm{d}\varphi] \exp\{\mathrm{i} A[j]\}$$

$$\equiv \prod_{n=-\infty}^{\infty} \left(\int_{\boldsymbol{x}} [\mathrm{d}\varphi_n] \right) \exp\{\mathrm{i} A[j]\} \tag{53}$$

where

$$A[j] \equiv \sum_{n=-\infty}^{\infty} F^n[j] = \sum_{n=-\infty}^{\infty} F^n_{(0)}[j] - \mathrm{i} \int_{n\lambda\boldsymbol{x}} V(\tilde{\varphi}_n) \tag{54}$$

and the φ_n are functionally integrated over their spatially-indexed degrees of freedom. In the above and subsequently we shall use the notation

$$\int_{n\lambda\boldsymbol{x}} \equiv T \int_0^1 \mathrm{d}\lambda \sum_{n=-\infty}^{\infty} \int \mathrm{d}^3 \boldsymbol{x} \tag{55}$$

whenever such a particular combination of spatial integration, summation, and virtual path integration occurs. This replaces the four-dimensional integral $\int \mathrm{d}^4 x \equiv \int \mathrm{d}t \, \mathrm{d}^3 \boldsymbol{x}$ found in normal relativistic field theory.

We now postulate our quantum dynamics to be governed by the equation

$$\int [\mathrm{d}\varphi] \left[\frac{\delta}{\varphi_n(\boldsymbol{x})} \{F^n + F^{n-1}\} + T j_n(\boldsymbol{x}) \right] \exp\{\mathrm{i}A[j]\} = 0 \qquad (56)$$

which is equivalent to a vacuum expectation value of the Heisenberg operator equations of motion derived formally from Cadzow's equation (2). Integrating by parts, we arrive at the more convenient expression

$$Z[j] = \exp\left\{ -\mathrm{i}\oint_{n\lambda\boldsymbol{x}} V(\mathcal{D}_{n\lambda\boldsymbol{x}}) \right\} Z_0[j] \qquad (57)$$

where

$$Z_0[j] \equiv \int [\mathrm{d}\varphi] \exp\left\{ \mathrm{i}T \sum_{n=-\infty}^{\infty} \int \mathrm{d}^3\boldsymbol{x}\, (\mathcal{F}_0^n + j_n\varphi_n) \right\}$$

$$= Z_0[0] \exp\left\{ -\tfrac{1}{2}\mathrm{i}T^2 \sum_{n,m=-\infty}^{\infty} \int \mathrm{d}^3\boldsymbol{x}\, \mathrm{d}^3\boldsymbol{y}\, j_n(\boldsymbol{x})\Delta_F^{n-m}(\boldsymbol{x}-\boldsymbol{y})j_m(\boldsymbol{y}) \right\} \qquad (58)$$

and

$$\mathcal{D}_{n\lambda\boldsymbol{x}} \equiv \frac{-\mathrm{i}}{T} U_n^\lambda \frac{\delta}{\delta j_n(\boldsymbol{x})}$$

$$= \frac{-\mathrm{i}}{T} \left\{ \lambda \frac{\delta}{\delta j_{n+1}(\boldsymbol{x})} + \bar{\lambda} \frac{\delta}{\delta j_n(\boldsymbol{x})} \right\}. \qquad (59)$$

Turning now to φ^3 theory, we recall that with hindsight the potential $V^{(3)}(\varphi)$ is normally taken to have the form

$$V^{(3)}(\varphi) = \frac{g}{3!}\{\varphi^3 - \Gamma\varphi\} \qquad (60)$$

where the (infinite) subtraction constant Γ is formally given by

$$\Gamma = 3\mathrm{i}\Delta_F(0). \qquad (61)$$

This has the role of cancelling out self-interaction loops at vertices in the Feynman rules expansion programme. We find that for discrete time, the same effect is achieved by taking the potential to have the form

$$V^{(3)}(\tilde{\varphi}_n) = \frac{g}{3!}\{\tilde{\varphi}_n^3 - \tilde{\Gamma}\tilde{\varphi}_n\} \qquad (62)$$

where

$$\tilde{\Gamma} = 2\mathrm{i}\Delta_F^0(\boldsymbol{0}) + \tfrac{1}{2}\mathrm{i}[\Delta_F^1(\boldsymbol{0}) + \Delta_F^{-1}(\boldsymbol{0})]. \qquad (63)$$

The first objective is to find a perturbative expansion for $Z[j]$, which we write in the form

$$Z[j] = Z_0[j] + Z_1[j] + Z_2[j] + \cdots \qquad (64)$$

where

$$Z_p[j] \equiv -\frac{\mathrm{i}}{p} \oint_{n\lambda\boldsymbol{x}} V^{(3)}(\mathcal{D}_{n\lambda\boldsymbol{x}})Z_{p-1}[j] \qquad p = 1, 2, \ldots. \qquad (65)$$

Having found $Z[j]$ we then calculate the required vacuum expectation value of time-ordered products of fields by functional differentiation in the standard way. The results lead to a set of rules for a diagrammatic expansion analogous to the Feynman rules in continuous time theory, with specific differences. The details of the calculations are omitted here as they are routine and tedious, but the results are as follows.

4.3. Feynman rules for discrete time-ordered products

The objective in this section is to present the rules for a diagrammatic expansion of scattering amplitudes in the absence of external sources. The latter are used merely to provide an internal handle on the correlation functions of the theory and are set to zero at the end of the day. This programme is carried out in two stages. In this section we give the rules for the evaluation of successive terms in a Feynman diagram type of expansion for the vacuum expectation value of the time-ordered product

$$\langle 0^{\text{out}}| \tilde{T} \hat{\varphi}_1(\boldsymbol{x}_1) \hat{\varphi}_2(\boldsymbol{x}_2) \dots \hat{\varphi}_k(\boldsymbol{x}_k)|0^{\text{in}}\rangle \tag{66}$$

with k discrete time scalar fields; we shall give the rules for a system with interaction given by (62), so the expansion is effectively in powers in the coupling constant g:

  (1) first find the ordinary continuous time Feynman rules in spacetime;

  (2) draw all the different diagrams normally discussed in this programme;

  (3) for a given diagram with V vertices and I internal lines find its conventional weighting factor ω, such as the well known factor of $\frac{1}{2}$ for the simple loop in φ^3 theory;

  (4) at each vertex, associate a factor

$$\mathrm{i}gT \oint_{m\lambda z} \equiv \mathrm{i}gT \int_0^1 \mathrm{d}\lambda \sum_{m=-\infty}^{\infty} \int \mathrm{d}^3 z \tag{67}$$

  (5) for each external line running from the external point $(n, \boldsymbol{x})$ to a vertex with indices $(m, \lambda, \boldsymbol{z})$ assign a propagator

$$\mathrm{i}U_m^\lambda \Delta_F^{m-n}(\boldsymbol{z} - \boldsymbol{x}) \tag{68}$$

  (6) for each internal line running from vertex $(m_1, \lambda_1, \boldsymbol{z}_1)$ to vertex $(m_2, \lambda_2, \boldsymbol{z}_2)$ assign a propagator

$$\mathrm{i}U_{m_1}^{\lambda_1} U_{m_2}^{\lambda_2} \Delta_F^{m_2-m_1}(\boldsymbol{z}_2 - \boldsymbol{z}_1) \tag{69}$$

  (7) apply the λ integrals.

It is in general much more convenient to perform the virtual path integrations (over the λ's) after the diagrams have been written down rather than before the diagrammatic expansion. In many cases the operator U_m^λ acting on an external propagator can be transferred to act on internal propagators using the rule

$$\sum_{m=-\infty}^{\infty} (U_m^\lambda f_m) g_m = \sum_{m=-\infty}^{\infty} f_m \bar{U}_m^\lambda g_m \tag{70}$$

for any indexed functions f_n, g_n, where we define

$$\bar{U}_m^\lambda g_m \equiv \lambda U_m^{-1} g_m + \bar{\lambda} g_m = \lambda g_{m-1} + \bar{\lambda} g_m. \tag{71}$$

However, this does not work so conveniently whenever two or more external lines meet at the same vertex.

To illustrate these rules in operation consider the conventional perturbation theory expansion of the time-ordered product $\langle 0|T\hat{\varphi}(x_1)\hat{\varphi}(x_2)|0\rangle$ in powers of the coupling constant. The conventional Feynman rules give the expansion

$$\langle 0|T\hat{\varphi}(x_1)\hat{\varphi}(x_2)|0\rangle = \mathrm{i}\Delta_F(x_1 - x_2) - \tfrac{1}{2}g^2 \int \mathrm{d}^4 z_1 \, \mathrm{d}^4 z_2 \, \Delta_F(x_1 - z_1)\Delta_F(z_1 - z_2)$$

$$\times \Delta_F(z_2 - z_1)\Delta_F(z_2 - x_2) + \mathrm{O}(g^4). \tag{72}$$

The second term on the right-hand side corresponds to the single loop diagram with $V = 2$, $I = 2$ in φ^3 scalar theory and is divergent. Part of the motivation for investigating discrete

time field theory is the hope that the corresponding diagram might be modified in some significant way.

Using the rules outlined above the analogue expansion in discrete time gives

$$\langle 0|\tilde{T}\hat{\varphi}_{n_1}(\boldsymbol{x}_1)\hat{\varphi}_{n_2}(\boldsymbol{x}_2)|0\rangle = \mathrm{i}\Delta_F^{n_1-n_2}(\boldsymbol{x}_1-\boldsymbol{x}_2) - \tfrac{1}{2}g^2 \oint_{m_1\lambda_1 z_1} \oint_{m_2\lambda_2 z_2} \{U_{m_1}^{\lambda_1}\Delta_F^{m_1-n_1}(\boldsymbol{z}_1-\boldsymbol{x}_1)\}$$

$$\times \{U_{m_1}^{\lambda_1}U_{m_2}^{\lambda_2}\Delta_F^{m_2-m_1}(\boldsymbol{z}_2-\boldsymbol{z}_1)\}\{U_{m_2}^{\lambda_2}U_{m_1}^{\lambda_1}\Delta_F^{m_1-m_2}(\boldsymbol{z}_1-\boldsymbol{z}_2)\}$$

$$\times \{U_{m_2}^{\lambda_2}\Delta_F^{m_2-n_2}(\boldsymbol{z}_2-\boldsymbol{x}_2)\} + \mathrm{O}(g^4). \tag{73}$$

For this particular process the second term on the right-hand side can be rewritten using the rule (70) to give

$$\langle 0|\tilde{T}\hat{\varphi}_{n_1}(\boldsymbol{x}_1)\hat{\varphi}_{n_2}(\boldsymbol{x}_2)|0\rangle = \mathrm{i}\Delta_F^{n_1-n_2}(\boldsymbol{x}_1-\boldsymbol{x}_2) - \tfrac{1}{2}g^2 \oint_{m_1\lambda_1 z_1} \oint_{m_2\lambda_2 z_2} \Delta_F^{m_1-n_1}(\boldsymbol{z}_1-\boldsymbol{x}_1)$$

$$\times \{\bar{U}_{m_1}^{\lambda_1}\bar{U}_{m_2}^{\lambda_2}[U_{m_1}^{\lambda_1}U_{m_2}^{\lambda_2}\Delta_F^{m_2-m_1}(\boldsymbol{z}_2-\boldsymbol{z}_1)]^2\}\Delta_F^{m_2-n_2}(\boldsymbol{z}_2-\boldsymbol{x}_2) + \mathrm{O}(g^4) \tag{74}$$

using the symmetry

$$\Delta_F^n(\boldsymbol{x}) = \Delta_F^{-n}(-\boldsymbol{x}). \tag{75}$$

The integrals over μ and λ can be integrated at this stage to give a multitude of subdiagrams distinguished by different split times, which is the ultimate effect of the discretization process. The various subdiagrams contributing to the loop diagram are shown in figure 1, each with a numerical factor. The sum over all numerical factors for this diagram should add up to 144. The full amplitude corresponding to the loop diagram is the sum of each of these subdiagrams, times the numerical factor for each subdiagram, divided by 288, taking into account the original weighting factor of $\tfrac{1}{2}$. By using symmetry arguments it can be shown that the 29 distinct diagrams in figure 1 reduce to the 12 diagrams shown in figure 2.

The above rules are relevant to vacuum expectation values of discrete time-ordered products of field operators. For particle scattering matrix elements the rules become simpler, as discussed next.

5. Scattering amplitudes

We are now in a position to discuss particle scattering amplitudes. First we explain how the scattering amplitude for a two–two particle scattering process based on the box diagram, figure 3, is calculated, and then we shall state the results for the general scattering diagram. This diagram was chosen because it involves a loop integration.

5.1. The two–two box scattering diagram

Consider two *incoming* scalar particles with 3-momenta $\boldsymbol{a}$, $\boldsymbol{b}$ respectively scattering via a the box scattering diagram shown in figure 3, into two *outgoing* particles with 3-momenta $\boldsymbol{c}$ and $\boldsymbol{d}$ respectively. Each of these particles is associated with a θ parameter as given by (45) which lies in the physical particle interval $[0, \pi)$. Negative values of such a parameter correspond to waves moving backwards in discrete time and would be interpreted in the usual way as antiparticles in the Feynman–Stueckelberg interpretation. Both positive and negative values occur in the discrete time Feynman propagators, just as in conventional field theory.
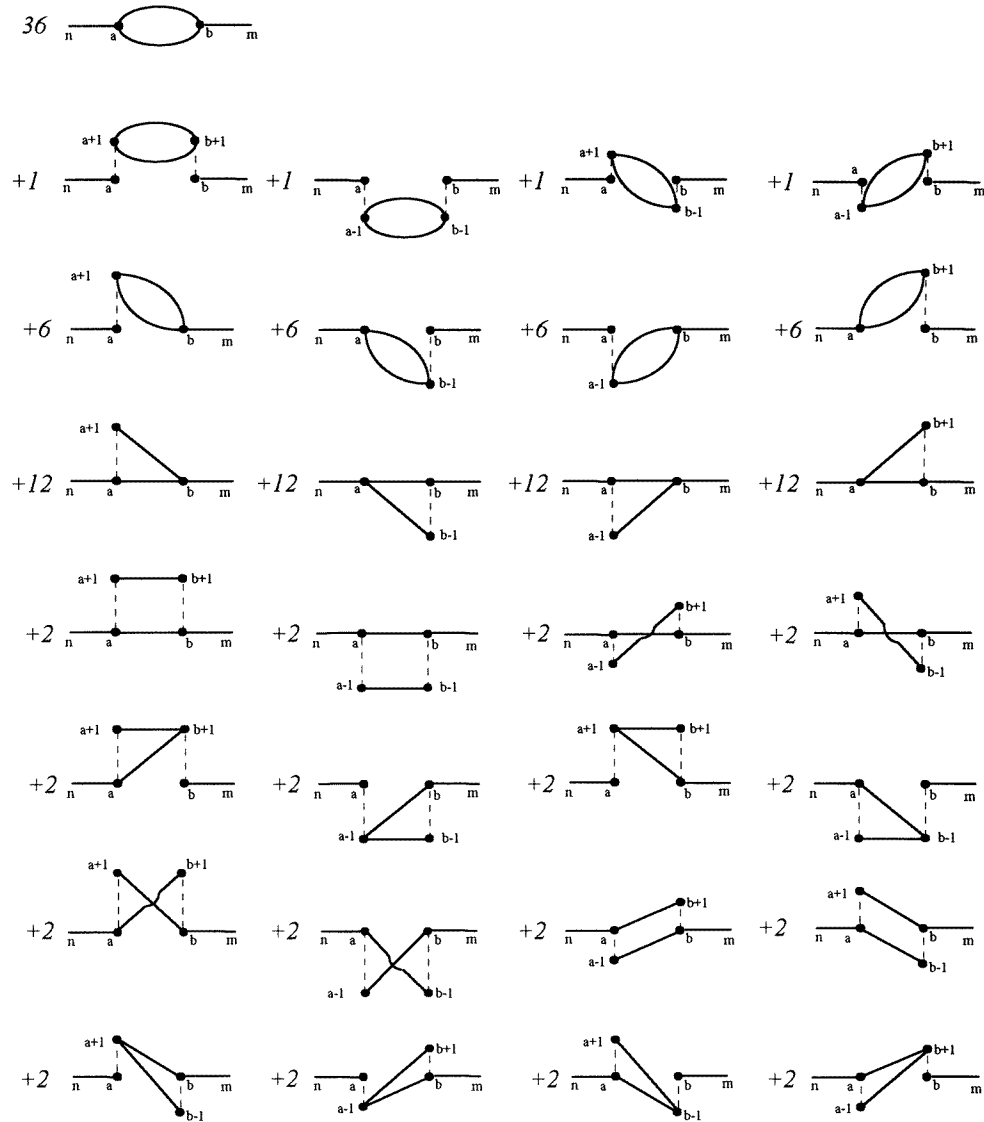
Figure 1. An expansion of the single-loop diagram in configuration space. There is a toal of 144 contributions, many of which can be equated and so we give the weighting for each type of contribution. The apparently disconnected pieces in most of these types arise because we have effectively split points in time when we wrote down the system function. In the limit $T \to 0$ these splits would collapse and all of these diagrams then reduce to 144 copies of the first type, corresponding to the conventional single-loop diagram.

Using the reduction formulae in section 4.1 we may write for the scattering reaction amplitude S_{if}

$$S_{if} \equiv \langle 0^{\text{out}}|\hat{a}_{\text{out}}(\boldsymbol{d})\hat{a}_{\text{out}}(\boldsymbol{c})\hat{a}_{\text{in}}^{+}(\boldsymbol{b})\hat{a}_{\text{in}}^{+}(\boldsymbol{a})|0^{\text{in}}\rangle_R$$

$$= \mathrm{i}^4\left(\prod_{j=1}^{4}\sum_{n_j=-\infty}^{\infty}\int \mathrm{d}^3\boldsymbol{x}_j\right)\mathrm{e}^{-\mathrm{i}n_1\theta_a+\mathrm{i}\boldsymbol{a}\cdot\boldsymbol{c}_1}\mathrm{e}^{-\mathrm{i}n_2\theta_b+\mathrm{i}\boldsymbol{b}\cdot\boldsymbol{x}_2}\mathrm{e}^{\mathrm{i}n_3\theta_c-\mathrm{i}\boldsymbol{c}\cdot\boldsymbol{x}_3}\mathrm{e}^{\mathrm{i}n_4\theta_d-\mathrm{i}\boldsymbol{d}\cdot\boldsymbol{x}_4}$$
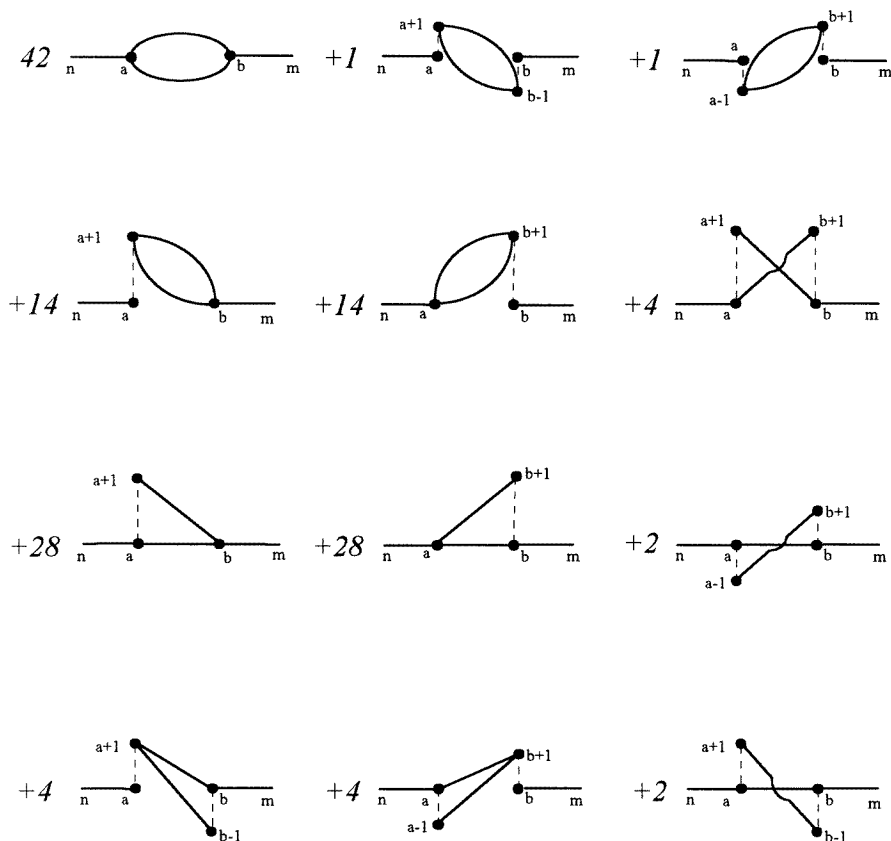
Figure 2. By using symmetry arguments, the various kinds of contributions shown in figure 1 can be simplified to the 12 varieties shown here. Again, the sum over all weightings is 144.
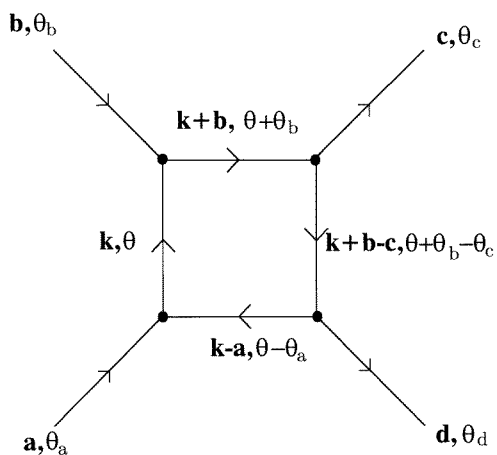

Figure 3. The two–two box scattering diagram used to illustrate the construction of the discrete time diagrammatic rules.

$$\times \overrightarrow{K_{n_1,a}}\overrightarrow{K_{n_2,b}}\overrightarrow{K_{n_3,c}}\overrightarrow{K_{n_4,d}}\langle 0^{\text{out}}|\tilde{T}\hat{\varphi}_{n_1}(\boldsymbol{x}_1)\hat{\varphi}_{n_2}(\boldsymbol{x}_2)\hat{\varphi}_{n_3}(\boldsymbol{x}_3)\hat{\varphi}_{n_4}(\boldsymbol{x}_4)|0^{\text{in}}\rangle \quad (76)$$

where

$$\overrightarrow{K_{n_1,a}} \equiv \Gamma^{-1}(\boldsymbol{a})(U_{n_1} - 2\eta(\boldsymbol{a}) + U_{n_1}^{-1}) \quad (77)$$

with

$$\Gamma(\boldsymbol{a}) \equiv \frac{6T}{6 + T^2 E_{\boldsymbol{a}}^2} \qquad E_{\boldsymbol{a}} \equiv \sqrt{\boldsymbol{a}\cdot\boldsymbol{a} + \mu^2} \qquad \eta(\boldsymbol{a}) \equiv \frac{6 - 2T^2 E_{\boldsymbol{a}}^2}{6 + T^2 E_{\boldsymbol{a}}^2} = \cos\theta_{\boldsymbol{a}} \quad (78)$$

and similarly for the other particles.

Next we expand the 4-point function according to the rules outlined in section 4.3 and consider for the purposes of this discussion only the contribution associated with the box diagram of figure 3, namely

$$\langle 0^{\text{out}}|\tilde{T}\hat{\varphi}_{n_1}(\boldsymbol{x}_1)\hat{\varphi}_{n_2}(\boldsymbol{x}_2)\hat{\varphi}_{n_3}(\boldsymbol{x}_3)\hat{\varphi}_{n_4}(\boldsymbol{x}_4)|0^{\text{in}}\rangle|_{\text{BOX}} = (\mathrm{i}gT)^4 \left(\prod_{j=1}^{4}\oint_{m_j\lambda_j z_j} \mathrm{i}U_{m_j}^{\lambda_j}\Delta_F^{m_j-n_j}(z_j - \boldsymbol{x}_j)\right)$$

$$\times [U_{m_2}^{\lambda_2}U_{m_1}^{\lambda_1}\Delta_F^{m_2-m_1}(z_2 - z_1)][U_{m_3}^{\lambda_3}U_{m_2}^{\lambda_2}\Delta_F^{m_3-m_2}(z_3 - z_2)]$$

$$\times [U_{m_4}^{\lambda_4}U_{m_3}^{\lambda_3}\Delta_F^{m_4-m_3}(z_4 - z_3)][U_{m_1}^{\lambda_1}U_{m_4}^{\lambda_4}\Delta_F^{m_1-m_4}(z_1 - z_4)]. \quad (79)$$

The next step is to do the $\boldsymbol{x}_j$ integrals, converting the 2-point functions on each external leg of the diagram to its momentum space form, using

$$\tilde{\Delta}_F^n(\boldsymbol{p}) = \int \mathrm{d}\boldsymbol{x}\, \mathrm{e}^{\mathrm{i}\boldsymbol{p}\cdot\boldsymbol{x}}\Delta_F^n(\boldsymbol{x}). \quad (80)$$

Then we use the result

$$\overrightarrow{K_{n,\boldsymbol{p}}}\tilde{\Delta}_F^n(\boldsymbol{p}) = -\delta_n \quad (81)$$

taking care to bring the operators and summations into the brackets whenever the U_m^λ operators occur. This effectively amputates the external legs of the diagram. Then we can immediately carry out the summations over the external integers n_i and arrive at the simplified form

$$S_{if} = (gT)^4 \left(\prod_{j=1}^{4}\sum_{m_j=-\infty}^{\infty}\int_0^1 \mathrm{d}\lambda_j \int \mathrm{d}^3 z_j\right)\mathrm{e}^{\mathrm{i}\boldsymbol{a}\cdot z_1 + \mathrm{i}\boldsymbol{b}\cdot z_2 - \mathrm{i}\boldsymbol{c}\cdot z_3 - \mathrm{i}\boldsymbol{d}\cdot z_4}$$

$$\times \{U_{m_1}^{\lambda_1}\mathrm{e}^{-\mathrm{i}m_1\theta_a}\}\{U_{m_2}^{\lambda_2}\mathrm{e}^{-\mathrm{i}m_2\theta_b}\}\{U_{m_3}^{\lambda_3}\mathrm{e}^{\mathrm{i}m_3\theta_c}\}\{U_{m_4}^{\lambda_4}\mathrm{e}^{\mathrm{i}m_4\theta_d}\}$$

$$\times [U_{m_2}^{\lambda_2}U_{m_1}^{\lambda_1}\Delta_F^{m_2-m_1}(z_2 - z_1)][U_{m_3}^{\lambda_3}U_{m_2}^{\lambda_2}\Delta_F^{m_3-m_2}(z_3 - z_2)]$$

$$\times [U_{m_4}^{\lambda_4}U_{m_3}^{\lambda_3}\Delta_F^{m_4-m_3}(z_4 - z_3)][U_{m_1}^{\lambda_1}U_{m_4}^{\lambda_4}\Delta_F^{m_1-m_4}(z_1 - z_4)]. \quad (82)$$

Now we use the representation of the propagator

$$\Delta_F^n(\boldsymbol{x}) \equiv \frac{1}{(2\pi)^4}\int \mathrm{d}^3\boldsymbol{k}\int_{-\pi}^{\pi}\frac{\mathrm{d}\theta}{T}\mathrm{e}^{-\mathrm{i}n\theta + \mathrm{i}\boldsymbol{k}\cdot\boldsymbol{x}}\tilde{\Delta}_F(\boldsymbol{k},\theta) \quad (83)$$

and evaluate the z_i integrals to find

$$S_{if} = g^4 (2\pi)^3 \delta^3(\boldsymbol{a} + \boldsymbol{b} - \boldsymbol{c} - \boldsymbol{d})\left(\prod_{j=1}^{4}\sum_{m_j=-\infty}^{\infty}\int_0^1 \mathrm{d}\lambda_j \frac{1}{2\pi}\int_{-\pi}^{\pi}\mathrm{d}\theta_j\right)$$

$$\times \int \frac{\mathrm{d}^3\boldsymbol{k}}{(2\pi)^3}\{U_{m_1}^{\lambda_1}\mathrm{e}^{-\mathrm{i}m_1\theta_a}\}\{U_{m_2}^{\lambda_2}\mathrm{e}^{-\mathrm{i}m_2\theta_b}\}\{U_{m_3}^{\lambda_3}\mathrm{e}^{\mathrm{i}m_3\theta_c}\}\{U_{m_4}^{\lambda_4}\mathrm{e}^{\mathrm{i}m_4\theta_d}\}$$

$$\times [U_{m_2}^{\lambda_2}U_{m_1}^{\lambda_1}\mathrm{e}^{-\mathrm{i}(m_2-m_1)\theta_1}\tilde{\Delta}_F(\boldsymbol{k},\theta_1)][U_{m_3}^{\lambda_3}U_{m_2}^{\lambda_2}\mathrm{e}^{-\mathrm{i}(m_3-m_2)}\tilde{\Delta}_F(\boldsymbol{k}+\boldsymbol{b},\theta_2)]$$

$$\times [U_{m_4}^{\lambda_4}U_{m_3}^{\lambda_3}\mathrm{e}^{-\mathrm{i}(m_4-m_3)}\tilde{\Delta}_F(\boldsymbol{k}+\boldsymbol{b}-\boldsymbol{c},\theta_3)][U_{m_1}^{\lambda_1}U_{m_4}^{\lambda_4}\mathrm{e}^{-\mathrm{i}(m_1-m_4)}\tilde{\Delta}_F(\boldsymbol{k}-\boldsymbol{a},\theta_4)]. \quad (84)$$

Here we see the appearance of overall linear momentum conservation, as expected. Next we use the result

$$U_m^\lambda e^{im\theta} = e^{im\theta} f_\lambda(\theta) \tag{85}$$

where

$$f_\lambda(\theta) \equiv \lambda e^{i\theta} + \bar{\lambda} \tag{86}$$

to find

$$S_{if} = g^4 (2\pi)^3 \delta^3(\boldsymbol{a} + \boldsymbol{b} - \boldsymbol{c} - \boldsymbol{d}) \left(\prod_{j=1}^4 \sum_{m_j=-\infty}^{\infty} \int_0^1 d\lambda_j \frac{1}{2\pi} \int_{-\pi}^{\pi} d\theta_j \right)$$

$$\times \int \frac{d^3\boldsymbol{k}}{(2\pi)^3} e^{-im_1\theta_a} f_{\lambda_1}^*(\theta_a) e^{-im_2\theta_b} f_{\lambda_2}^*(\theta_b) e^{im_3\theta_c} f_{\lambda_3}(\theta_c) e^{im_4\theta_d} f_{\lambda_4}(\theta_4)$$

$$\times e^{i(m_1-m_2)\theta_1} f_{\lambda_1}(\theta_1) f_{\lambda_2}^*(\theta_1) \tilde{\Delta}_F(\boldsymbol{k}, \theta_1) e^{i(m_2-m_3)\theta_2} f_{\lambda_2}(\theta_2) f_{\lambda_3}^*(\theta_2) \tilde{\Delta}_F(\boldsymbol{k} + \boldsymbol{b}, \theta_2)$$

$$\times e^{i(m_3-m_4)\theta_3} f_{\lambda_3}(\theta_3) f_{\lambda_4}^*(\theta_3) \tilde{\Delta}_F(\boldsymbol{k} + \boldsymbol{b} - \boldsymbol{c}, \theta_3)$$

$$\times e^{i(m_4-m_1)\theta_4} f_{\lambda_4}(\theta_4) f_{\lambda_1}^*(\theta_4) \tilde{\Delta}_F(\boldsymbol{k} - \boldsymbol{a}, \theta_4). \tag{87}$$

We are now able to perform the summations over the m_i. We notice that each summation gives a Fourier series representation of the periodic Dirac delta, namely

$$\sum_{m=-\infty}^{\infty} e^{imx} = 2\pi \sum_{m=-\infty}^{\infty} \delta(x + 2m\pi) \equiv 2\pi \delta_P(x) \tag{88}$$

and so we find

$$S_{if} = g^4 (2\pi)^4 \delta_P(\theta_a + \theta_b - \theta_c - \theta_d) \delta^3(\boldsymbol{a} + \boldsymbol{b} - \boldsymbol{c} - \boldsymbol{d}) \left(\prod_{j=1}^4 \int_0^1 d\lambda_j \right)$$

$$\times \int \frac{d^3\boldsymbol{k}}{(2\pi)^4} \int_{-\pi}^{\pi} d\theta \, f_{\lambda_1}^*(\theta_a) f_{\lambda_2}^*(\theta_b) f_{\lambda_3}(\theta_c) f_{\lambda_4}(\theta_4) f_{\lambda_1}(\theta) f_{\lambda_2}^*(\theta) \tilde{\Delta}_F(\boldsymbol{k}, \theta)$$

$$\times f_{\lambda_2}(\theta + \theta_b) f_{\lambda_3}^*(\theta + \theta_b) \tilde{\Delta}_F(\boldsymbol{k} + \boldsymbol{b}, \theta + \theta_b) f_{\lambda_3}(\theta + \theta_b - \theta_c)$$

$$\times f_{\lambda_4}^*(\theta + \theta_b - \theta_c) \tilde{\Delta}_F(\boldsymbol{k} + \boldsymbol{b} - \boldsymbol{c}, \theta + \theta_b - \theta_c) f_{\lambda_4}(\theta - \theta_a)$$

$$\times f_{\lambda_1}^*(\theta - \theta_a) \tilde{\Delta}_F(\boldsymbol{k} - \boldsymbol{a}, \theta - \theta_a). \tag{89}$$

The crucial significance of this step is that we see the appearance of a conservation rule for the parameters θ. This is despite the non-existence of a Hamiltonian in our formulation and the fact that we have not constructed a Logan invariant for the fully interacting system.

We may go further and apply the λ_i integrals. We define the *vertex function*

$$V(\theta_a, \theta_b) \equiv \int_0^1 d\lambda \, f_\lambda^*(\theta_a) f_\lambda^*(\theta_b) f_\lambda(\theta_a + \theta_b)$$

$$= \frac{\cos(\theta_a + \theta_b) + \cos(\theta_a) + \cos(\theta_b) + 3}{6} \tag{90}$$

and so get the final result

$$S_{if} = g^4 (2\pi)^4 \delta_P(\theta_a + \theta_b - \theta_c - \theta_d) \delta^3(\boldsymbol{a} + \boldsymbol{b} - \boldsymbol{c} - \boldsymbol{d})$$

$$\times \int \frac{d^3\boldsymbol{k}}{(2\pi)^4} \int_{-\pi}^{\pi} d\theta \, V(\theta_a, -\theta) V(\theta_b, \theta) V(\theta + \theta_b, -\theta_c) V(-\theta_d, \theta_a - \theta)$$

$$\times \tilde{\Delta}_F(\boldsymbol{k}, \theta) \tilde{\Delta}_F(\boldsymbol{k} + \boldsymbol{b}, \theta + \theta_b) \tilde{\Delta}_F(\boldsymbol{k} + \boldsymbol{b} - \boldsymbol{c}, \theta + \theta_b - \theta_c)$$

$$\times \tilde{\Delta}_F(\boldsymbol{k} - \boldsymbol{a}, \theta - \theta_a). \tag{91}$$
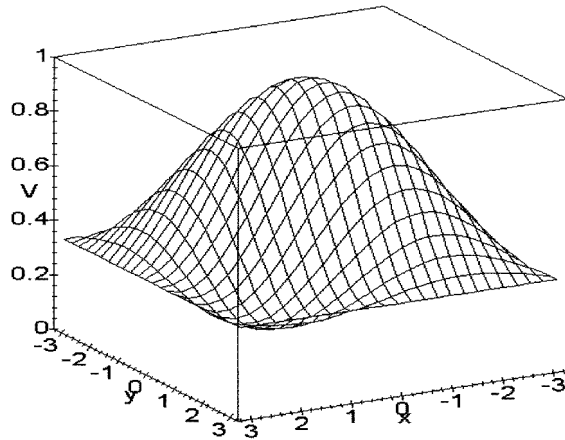
Figure 4. A plot of the vertex function $V(x, y)$, where each argument lies in the interval $[-\pi, \pi]$. The vertex function takes its maximum value of unity when $x = y = 0$, which corresponds to the continuous time limit $T \to 0$. The vertex function never falls below the value $\frac{1}{4}$.

A diagrammatic representation of the above shows that θ-conservation occurs at every vertex.

5.2. The vertex functions

The vertex functions $V(\theta_1, \theta_2)$ represent a degree of softening at each vertex arising from our temporal point splitting via the system function. At each vertex the sum of the *incoming* θ parameters is always zero, including inside loops, so the vertex function always depends on two parameters only. If we had a φ^4 interaction we expect the vertex function will depend on three parameters, and so on. A graphical presentation of the vertex function is given in figure 4. The vertex function has a minimum value of one quarter and attains its maximum value of unity when the θ parameters are each zero. This corresponds to the continuous time limit $T \to 0$.

5.3. The propagators

The propagators used in the final amplitude (91) are readily found using the basic definition

$$\tilde{\Delta}_F(\boldsymbol{p}, \theta) \equiv T \sum_{n=-\infty}^{\infty} e^{in\theta} \tilde{\Delta}_F^n(\boldsymbol{p}) \tag{92}$$

and the equation

$$(U_n - 2\eta_E + U_n^{-1})\tilde{\Delta}_F^n(\boldsymbol{p}) = -\Gamma_E \delta_n \tag{93}$$

then

$$2(\cos\theta - \eta_E)\tilde{\Delta}_F(\boldsymbol{p}, \theta) = -T\Gamma_E. \tag{94}$$

Now we need to choose the correct solution for Feynman scattering boundary conditions. This is done by referring to the Feynman $-i\epsilon$ prescription, which corresponds to the replacement of E^2 in the above by $E^2 - i\epsilon$. This in turn corresponds to the replacement

$$\eta_E \to \eta_E + i\epsilon. \tag{95}$$

Hence we arrive at the desired solution

$$\tilde{\Delta}_F(\boldsymbol{p}, \theta) = \frac{-T\Gamma_E}{2(\cos\theta - \eta_E - i\epsilon)} \tag{96}$$

which holds for both the elliptic region $-1 < \eta_E < 1$ and for the hyperbolic region $-2 < \eta_E < -1$. It may be verified that the indexed propagators (23) are given by the integrals

$$\tilde{\Delta}_F^n(\boldsymbol{p}) = \frac{1}{2\pi} \int_{-\theta}^{\theta} d\theta\, e^{-in\theta} \frac{-\Gamma_E}{2(\cos\theta - \eta_E - i\epsilon)}$$
$$= \frac{\Gamma_E}{2\pi i} \oint \frac{dz}{z^n(z^2 - 2(\eta_E + i\epsilon)z + 1)} \tag{97}$$

the contour of integration being the unit circle in the anticlockwise sense. We find for example

$$\tilde{\Delta}_F^n(\boldsymbol{p}) = \frac{\Gamma_E}{2i\sin\theta_E} e^{-i|n|\theta_E} \tag{98}$$

in the case of the elliptic regime, $T^2 E^2 < 12$, and

$$\tilde{\Delta}_F^n(\boldsymbol{p}) = \frac{(-1)^{n+1}\Gamma_E}{2\sinh\gamma_E} e^{-|n|\gamma_E} \tag{99}$$

in the hyperbolic regime, $T^2 E^2 > 12$. Here we make the parametrization

$$\cos(\zeta) \equiv \eta_E = \frac{6 - 2T^2 E^2}{6 + T^2 E^2} \tag{100}$$

where ζ is a complex parameter running just below the real axis from the origin to π (when ζ is written as θ_E) and then from π to $\pi - i\ln(2 + \sqrt{3})$ (when ζ is written in the form $\pi - i\gamma_E$).

If in (96) we introduce the variable p_0 related to θ by the rule

$$\cos\theta \equiv \frac{6 - 2p_0^2 T^2}{6 + p_0^2 T^2} \qquad \text{sign}(\theta) = \text{sign}(p_0) \tag{101}$$

then we find

$$\tilde{\Delta}_F(\boldsymbol{p}, \theta) = \frac{1}{p_0^2 - \boldsymbol{p}^2 - m^2 + i\epsilon} + \frac{T^2 p_0^2}{6(p_0^2 - \boldsymbol{p}^2 - m^2 + i\epsilon)} \tag{102}$$

an exact result. From this we see the emergence of Lorentz symmetry as an approximate symmetry of the mechanics. If p_0 in the above is taken to represent the zeroth component of a four vector, with the components of $\boldsymbol{p}$ representing the remaining components, then we readily see that the first term on the right-hand side of (102) is Lorentz invariant. The second term is not Lorentz invariant, but we note it is proportional to T^2. If, as we expect, T represents an extremely small scale, such as the Planck time or less, then it is clear that Lorentz symmetry should emerge as an extremely good approximate symmetry of our mechanics.

5.4. Comments

The significance of our results is that not only is spatial momentum conserved during a scattering process, as expected from the Maeda–Noether [1, 9] theorem, but the sum of the θ parameters of the incoming particles is conserved. This is the discrete time analogue of energy conservation, since in the limit $T \to 0$ we note

$$\lim_{T \to 0} \frac{\theta_p}{T} = E_p = \sqrt{\boldsymbol{p} \cdot \boldsymbol{p} + \mu^2}. \tag{103}$$

The θ conservation rule is unexpected at first sight in that we have not discussed as yet any Logan invariant for the full interacting system function. It appears that the analogue of energy conservation occurs here because of the way in which we have set up our incoming and outgoing states and allowed the scattering process to take place over infinite time. The result would probably not hold for scattering over finite time intervals, which would be the analogue of the time-energy uncertainty relation in conventional quantum theory. In essence, the LSZ scattering postulates relate the Logan invariant for *in*-states to the Logan invariant for the *out*-states in such a way that knowledge of the Logan invariant for the intermediate time appears not to be required. This is true of the scattering formalism as we have demonstrated, but the bound state question would be a different matter.

Although the conservation of θ-parameters during scattering processes comes as a surprise it is a welcome one. Before the calculations were performed explicitly, it was believed that the energy conservation rule in continuous time scattering processes would only arise in the limit $T \to 0$. Such a phenomenon was discussed by Lee [11] in his discrete time mechanics, which differs from ours in that his time intervals are determined by the dynamics. That there is an exact conservation rule for *something* in our discrete time scattering processes regardless of the magnitude of T is an indicator of the existence of some Logan invariant. The surprise is that the something turns out to be the sum of the incoming θ parameters, which suggests that our parametrization of the harmonic oscillator discussed in *paper I* was a fortuitously good one.

We point out here that our parameter θ is really an angle, unlike conventional energy E, or p_0 in the above, and there is an implied periodicity. However, because there is no concept of Hamiltonian or energy in our theory, this periodicity does not cause any physically relevant side effects. Incoming or outgoing particles will be *on-shell* in the sense that their associated θ parameter can be restricted to take a value in the interval $[0, \pi)$. Given this, we may then invert (101) to find

$$\theta = p_0 T - \frac{1}{24} p_0^3 T^3 + O(T^5). \tag{104}$$

Another welcome feature is the modification of the propagators and the appearance of vertex softening in the scattering diagrams. A detailed discussion of the effects these features have on the divergences of various loop integrals found in the conventional Feynman diagram programme will be reserved for a subsequent paper.

The scattering amplitude found above for figure 3 reduces to the correct continuous time amplitude in the limit $T \to 0$.

5.5. Rules for scattering amplitudes

We are now in a position to use our experience with the box diagram figure 3 to write down the general rules for scattering diagrams. Consider a scattering process with a incoming particles with momenta $\boldsymbol{p}_1, \boldsymbol{p}_2, \dots, \boldsymbol{p}_a$ respectively, and b outgoing particles with momenta

$q_1, q_2, \ldots q_b$ respectively. Make a diagrammatic expansion in the traditional manner of Feynman. For each diagram do the following:

(1) at each vertex, conserve linear momentum and θ parameters, i.e. the algebraic sum of *incoming* momenta is zero and the algebraic sum of the *incoming* θ parameters is zero;

(2) at each vertex associate a factor

$$\mathrm{i}gTV(\theta_1, \theta_2) \tag{105}$$

where θ_1 and θ_2 are any two of the three *incoming* θ parameters;

(3) for each internal line carrying momentum $\mathbf{k}$ and θ parameter, associate a factor

$$\mathrm{i}T^{-1}\tilde{\Delta}_F(\mathbf{k}, \theta) \tag{106}$$

(4) for each loop integral, a factor

$$\int \frac{\mathrm{d}^3\mathbf{k}}{(2\pi)^4} \int_{-\pi}^{\pi} \mathrm{d}\theta \tag{107}$$

(5) an overall momentum-θ parameter conservation factor

$$(2\pi)^4\delta_P(\theta_{p_1} + \cdots + \theta_{p_a} - \theta_{q_1} - \cdots \theta q_b)\delta^3(\mathbf{p}_1 + \cdots + \mathbf{p}_a - \mathbf{q}_1 - \cdots - \mathbf{q}_b) \tag{108}$$

(6) a weight factor ω for each diagram, exactly as for the standard Feynman rules.

6. Examples

We are now in a position to give a number of examples of scattering amplitude calculations using the above rules. We restrict our attention to φ^3 theory as an illustrative example. QED and the associated discrete time Feynman rules will be the subject of the next paper in this series, *paper IV*.

6.1. Figure 5(a)

Consider the basic single vertex diagram of figure 5(a) with particles with linear momentum $\mathbf{a}, \mathbf{b}$ fusing to form a particle with linear momentum $\mathbf{c}$. Overlooking the fact that this process gives zero for on-shell momenta our discrete time Feynman rules give

$$S_{5a} = \mathrm{i}gT(2\pi)^4\delta_P(\theta_a + \theta_b - \theta_c)\delta^3(\mathbf{a} + \mathbf{b} - \mathbf{c})V(\mathbf{a}, \mathbf{b}). \tag{109}$$

6.2. Figure 5(b)

This diagram has a single loop. We find

$$S_{5b} = -g^3(2\pi)^4\delta_P(\theta_a + \theta_b - \theta_c)\delta^3(\mathbf{a} + \mathbf{b} - \mathbf{c})$$
$$\times \int \frac{\mathrm{d}^3\mathbf{k}}{(2\pi)^4} \int_{-\pi}^{\pi} \mathrm{d}\theta\, V(\theta_a, -\theta)V(\theta_b, \theta - \theta_c)V(-\theta_c, \theta)\, \tilde{\Delta}_F(\mathbf{k}, \theta)$$
$$\times \tilde{\Delta}_F(\mathbf{k} - \mathbf{c}, \theta - \theta_c)\tilde{\Delta}_F(\mathbf{k} - \mathbf{a}, \theta - \theta_a). \tag{110}$$

The nature of this diagram will be discussed in detail in subsequent papers.
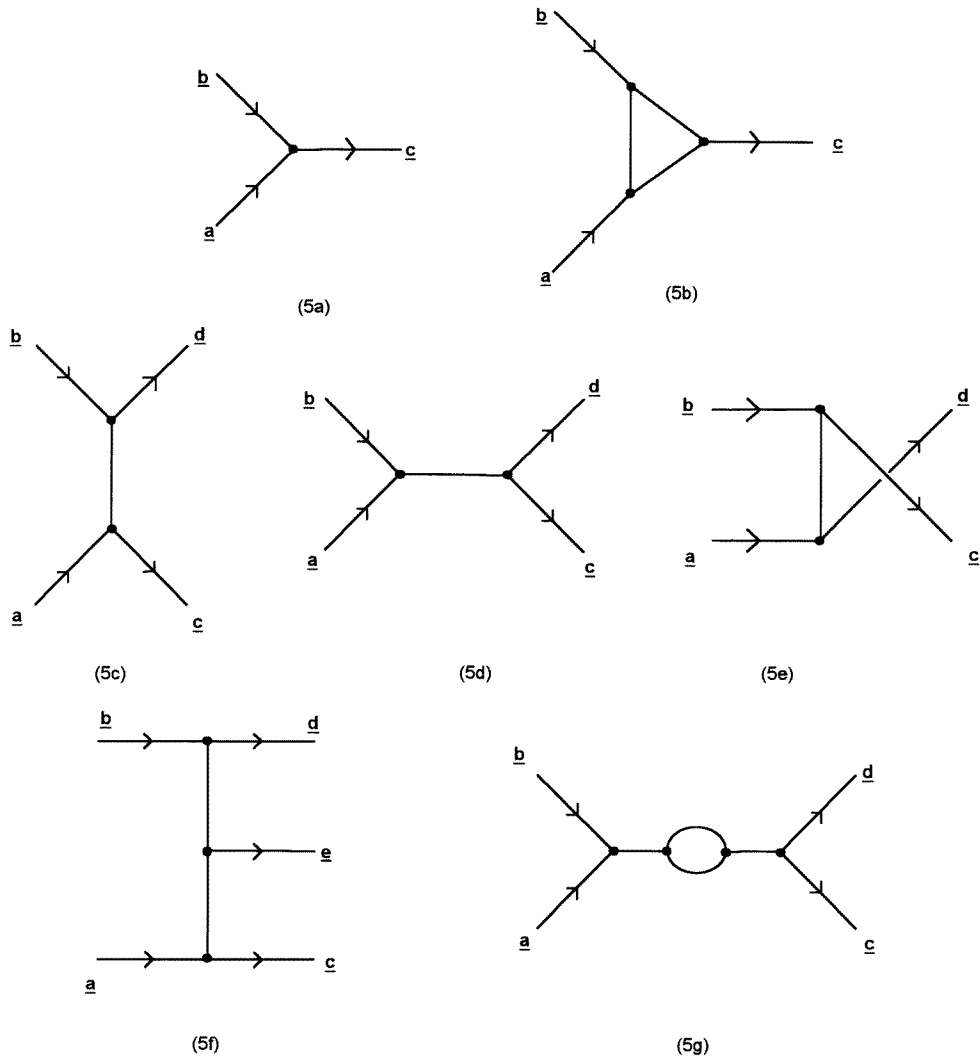
Figure 5. A number of diagrams to which our discrete time scattering rules have been applied.

6.3. Figures 5(c)–(e)

The order g^2 two–two scattering diagrams figures $5(c)$–(e) give

$$
\begin{aligned}
S_{5cde} = -g^2 T (2\pi)^4 \delta_P (\theta_a + \theta_b - \theta_c - \theta_d) \delta^3 (\boldsymbol{a} + \boldsymbol{b} - \boldsymbol{c} - \boldsymbol{d}) \\
\times \{ V(\theta_a, -\theta_c) V(\theta_b, -\theta_d) \tilde{\Delta}_F (\boldsymbol{a} - \boldsymbol{c}, \theta_a - \theta_c) \\
+ V(\theta_a, \theta_b) V(-\theta_c, -\theta_d) \tilde{\Delta}_F (\boldsymbol{a} + \boldsymbol{b}, \theta_a + \theta_b) \\
+ V(\theta_a, -\theta_d) V(\theta_b, -\theta_c) \tilde{\Delta}_F (\boldsymbol{a} - \boldsymbol{d}, \theta_a - \theta_d) \}.
\end{aligned}
\tag{111}
$$

6.4. Figure 5(f)

This diagram is an example of a higher-order tree diagram process involving no loops. We find

$$S_{5f} = \mathrm{i}g^3 T (2\pi)^4 \delta_P(\theta_a + \theta_b - \theta_c - \theta_d - \theta_e)\delta^3(\boldsymbol{a} + \boldsymbol{b} - \boldsymbol{c} - \boldsymbol{d} - \boldsymbol{e})$$
$$\times V(\theta_a, -\theta_c)V(\theta_b, -\theta_d)V(\theta_a - \theta_c, \theta_b - \theta_d)$$
$$\times \tilde{\Delta}_F(\boldsymbol{a} - \boldsymbol{c}, \theta_a - \theta_c)\tilde{\Delta}_F(\boldsymbol{d} - \boldsymbol{b}, \theta_d - \theta_b). \tag{112}$$

6.5. Figure 5(g)

This diagram has a simple propagator loop and gives

$$S_{5g} = \tfrac{1}{2}g^4(2\pi)^4 \delta_P(\theta_a + \theta_b - \theta_c - \theta_d)\delta^3(\boldsymbol{a} + \boldsymbol{b} - \boldsymbol{c} - \boldsymbol{d})\tilde{\Delta}_F(\boldsymbol{a} + \boldsymbol{b}, \theta_a + \theta_b)$$
$$\times \left\{ \frac{1}{(2\pi)^4} \int \mathrm{d}^3\boldsymbol{k} \int_{-\theta}^{\theta} \mathrm{d}\theta\; V(\theta_a, \theta_b)V(\theta_a + \theta_b, -\theta)V(\theta, -\theta_a - \theta_b) \right.$$
$$\left. \times V(-\theta_c - \theta_d)\tilde{\Delta}_F(\boldsymbol{k}, \theta)\tilde{\Delta}(\boldsymbol{k} - \boldsymbol{a} - \boldsymbol{b}, \theta - \theta_c - \theta_d) \right\} \tilde{\Delta}_F(\boldsymbol{a} + \boldsymbol{b}, \theta_a + \theta_b). \tag{113}$$

The question of the divergence of this integral will be reserved for a subsequent paper.

7. Concluding remarks

The application of the principles outlines in *papers I* and II to scalar field theory has indicated that the conventional programme of constructing Feynman rules for scattering amplitudes goes over well into discrete time. Of course there are differences, and it is to be hoped that some of these will alleviate if not overcome some of the divergence problems of the conventional field theory programme. An important point is that there occurs in our approach a natural scale provided by T. It is possible that this will provide a renormalization cutoff scale which will not have to be introduced by hand. Issues of renormalization and divergence will be discussed in a later paper.

   A particularly important result which was not anticipated before the diagrams were calculated is the conservation of the total θ parameters over a scattering process. This occurs even though no Logan invariant corresponding to the total Hamiltonian has been found for the fully interacting theory.

   An important point to consider is the question of relativistic covariance. Clearly our process of temporal discretization breaks Lorentz covariance, and with it the Poincaré algebra. However, it should be admitted by any critic that there is actually no empirical evidence that special relativity holds all the way up to infinite momentum. It is only an abstraction from limited experience that it does. Therefore, the Poincaré algebra has no more than the status of a really useful synthesis of limited experience. By requiring our parameter T to be small enough we should be able to reproduce all of the good predictions of continuous time mechanics, with the possibility of alleviating, if not removing, those aspects which are known to cause problems, such as divergences in the renormalization programme. Moreover, we have given a principle based on the cosmic background radiation field for finding a unique local inertial frame in which time is discretized.

   Finally, if our discrete time programme could be caught out in a fatal way, then we would have what amounts to a proof that time is really continuous. This in itself makes our investigation a worthwhile one.

Acknowledgment

References

[1] Jaroszkiewicz G and Norton K 1997 Principles of discrete time mechanics: I. Particle systems *J. Phys. A: Math. Gen.* **30** 3115–44
[2] Jaroszkiewicz G and Norton K 1997 Principles of discrete time mechanics: II. Classical field theory *J. Phys. A: Math. Gen.* **30** 3145–63
[3] Bender C M, Mead L R and Milton K A 1993 Discrete time quantum mechanics *Preprint* electronic archives http://xxx.lanl.gov.hep-ph/9305246
[4] Yamamoto H *et al* 1995 Conserved quantities of field theory on discrete spacetime *Prog. Theor. Phys.* **93** 173–84
[5] Guth A H 1989 Starting the universe: the big bang and cosmic inflation *Bubbles, Voids and Bumps in Time: The New Cosmology* ed J Cornwell (Cambridge: Cambridge University Press) pp 105–46
[6] Wright E L *et al* 1992 Interpretation of the CMB anisotropy detected by the COBE DMR *Astrophys. J.* **396** L13–18
[7] Nodland B and Ralston J P 1997 Indication of anisotropy in electromagnetic propagation over cosmological distances *Phys. Rev. Lett.* **78** 3043–6
[8] Cadzow J A 1970 Discrete calculus of variations *Int. J. Control* **11** 393–407
[9] Maeda S 1981 Extension of discrete Noether theorem *Math. Japonica* **26** 85–90 and references therein.
[10] Logan J D 1973 First integrals in the discrete variational calculus *Aequat. Math.* **9** 210–20
[11] Lee T D 1983 Can time be a discrete dynamical variable? *Phys. Lett.* **122B** 217–20